Supplemental Material

Journal of Climate
Revisiting the Inconsistent Influence of El Niño–Southern Oscillation on the Equatorial Atlantic
https://doi.org/10.1175/JCLI-D-24-0182.1

Table 1. Model information about the CMIP6 piControl simulations used in this study.

Model name	Country /Region	Atmosphere model Atmospheric resolution	Ocean model Oceanic resolution	Analyzed period (years)
ACCESS-CM2	Australia	MetUM-HadGEM3-GA7.1 N96 (~192˚ × 144˚); 85 levels	ACCESS-OM2 (GFDL-MOM5) tripolar primarily 1 ˚; 50 levels	500
ACCESS-ESM1-5	Australia	HadGAM2 N96 (~192˚ x 145˚); 38 levels	ACCESS-OM2 (GFDL-MOM5) tripolar primarily 1 ˚; 50 levels	1000
AWI-CM-1-1-MR	Germany	ECHAM6.3.04p1 T127 (~0.94˚× 0.94˚); 95 levels	FESOM 1.4 Unstructured grid in the horizontal with 830305 wet nodes; 46 levels	500
BCC-CSM2-MR	China	BCC_AGCM3_MR T106 (~1.125˚× 1.125˚); 46 levels	MOM4 1/3˚ in 30˚S-30˚N, 1/3˚-1˚ in 30˚ - 60˚N/S, and 1˚ in high latitudes; 40 levels	600
BCC-ESM1	China	BCC_AGCM3_LR T42 (~2.8125˚× 2.8125˚); 26 levels	MOM4 1/3˚ in 10˚S-10˚N, 1/3˚-1˚ in 10˚ - 30˚N/S, and 1˚ in high latitudes; 40 levels	452
CAMS-CSM1-0	China	ECHAM5_CAMS T106 (~1.125˚× 1.125˚); 31 levels	MOM4 Primarily 1˚×1˚, and 1/3˚ in 30˚S-30˚N; 50 levels	250
CanESM5	Canada	CanAM5 T63 linear gaussian grid (~2.8125˚× 2.8125˚); 49 levels	NEMO3.4.1 1˚ with refinement to 1/3˚ in 20˚S-20˚N; 45 levels	1000
CESM2-WACCM	USA	CAM6 Finite volume grid (0.9˚×1.25˚); 70 levels	POP2 320x384 longitude/latitude; 60 levels	500
CESM2	USA	CAM6 Finite volume grid (0.9˚×1.25˚); 32 levels	POP2 320x384 longitude/latitude; 60 levels	1200
CIESM	China	CIESM-AM 1˚ (288 x 192); 30 levels	CIESM-OM 0.5˚ (720 x 560); 46 levels	500

Model name	Country /Region	Atmosphere model Atmospheric resolution	Ocean model Oceanic resolution	Analyzed period (years)
CNRM-CM6-1-HR	France	Arpege 6.3 T359 (~35km); 91 levels	NEMO3.6 Primarily 0.25˚; 1442 x 1050 longitude/latitude; 75 levels	300
CNRM-CM6-1	France	Arpege 6.3 T127 (~100km); 91 levels	NEMO3.6 Primarily 1˚; 362 x 294 longitude/latitude; 75 levels	500
CNRM-ESM2-1	France	Arpege 6.3 T127 (~100km); 91 levels	NEMO3.6 Primarily 1˚; 362 x 294 longitude/latitude; 75 levels	500
E3SM-1-0	USA	EAM v1.0 1˚ average grid spacing; 72 levels	MPAS-Ocean v6 Variable resolution 60 km to 30 km; 60 levels	500
E3SM-1-1	USA	EAM v1.1 1˚ average grid spacing; 72 levels	MPAS-Ocean v6 Variable resolution 60 km to 30 km; 60 levels	166
EC-Earth3-Veg	European countries	IFS cy36r4 TL255 (~70km); 91 levels	NEMO3.6 Primarily 1˚; 362 x 294 longitude/latitude; 75 levels	500
EC-Earth3	European countries	IFS cy36r4 TL255 (~70km); 91 levels	NEMO3.6 Primarily 1˚; 362 x 294 longitude/latitude; 75 levels	502
FGOALS-f3-L	China	FAMIL2.2 C96 (~1˚×1); 32 levels	LICOM3.0 Primarily 1˚; 360 x 218 longitude/latitude; 30 levels	562
FGOALS-g3	China	GAMIL2 180˚ x 90˚ (~200km); 26 levels	LICOM3.0 Primarily 1˚; 360 x 218 longitude/latitude; 30 levels	700
FIO-ESM-2-0	China	CAM4 0.9˚ x 1.25˚ finite volume; 26 levels	POP2-W Displaced pole; Primarily 1˚; 60 levels	300
GISS-E2-1-G-CC	USA	GISS-E2.1 2.5˚x2˚; 40 levels	GISS Ocean 1.25˚x1˚; 32 levels	166

Model name	Country /Region	Atmosphere model Atmospheric resolution	Ocean model Oceanic resolution	Analyzed period (years)
GISS-E2-1-G	USA	GISS-E2.1 2.5˚x2˚; 40 levels	GISS Ocean 1.25˚x1˚; 32 levels	852
GISS-E2-1-H	USA	GISS-E2.1 2.5˚x2˚; 40 levels	HYCOM Ocean ~1˚×1˚; 26 levels	402
HadGEM3-GC31-LL	UK	MetUM-HadGEM3-GA7.1 N96 (1.875˚x1.25˚); 85 levels	NEMO-HadGEM3-GO6.0 Primarily 1˚ with meridional refinement down to 1/3 ˚ in the tropics; 75 levels	500
HadGEM3-GC31-MM	UK	MetUM-HadGEM3-GA7.1 N216 (~0.83˚x0.55˚); 85 levels	NEMO-HadGEM3-GO6.0 Primarily 0.25˚; 1440 x 1205 longitude/latitude; 75 levels	500
ICON-ESM-LR	Germany	ICON-A icosahedral/triangles; 160 km; 47 levels	ICON-O icosahedral/triangles; 40 km; 40 levels	500
IITM-ESM	India	IITM-GFSv1 T62L64 (192˚ x 94˚); 64 levels	MOM4p1 tripolar, primarily 1˚; 50 levels	200
INM-CM5-0	Russia	INM-AM4-8 2˚ x 1.5˚; 21 levels	INM-OM5 North Pole shifted to 60˚ N, 90˚E; 0.5˚ x 0.25˚; 40 levels	1202
IPSL-CM6A-LR	France	LMDZ N96 (2.5˚x1.259˚); 79 levels	NEMO-OPA Primarily 1˚; 75 levels	1200
KACE-1-0-G	South Korea	MetUM-HadGEM3-GA7.1 N96 (~ 192˚ x 144˚); 85 levels	MOM4p1 tripolar primarily 1˚; 50 levels	450
KIOST-ESM	South Korea	GFDL-AM2.0 C48 (192 x 96); 32 vertical levels	GFDL-MOM5.0 (tripolar - nominal 1˚; 52 levels	650
MCM-UA-1-0	USA	R30L14 3.75˚ x 2.5˚; 14 levels	MOM1.0 1.875 ˚x 2.5˚; 18 levels	500
MIROC-ES2L	Japan	CCSR AGCM T42 (~2.8125˚× 2.8125˚); 42 levels	COCO4.9 Primarily 1˚; 360 x 256 longitude/latitude; 63 levels	500

Model name	Country /Region	Atmosphere model Atmospheric resolution	Ocean model Oceanic resolution	Analyzed period (years)
MIROC6	Japan	CCSR AGCM T85 (~1.4°× 1.4°); 81 levels	COCO4.9 Primarily 1˚; 360 x 256 longitude/latitude; 63 levels	800
MPI-ESM1-2-HR	Germany	ECHAM6.3 T127 (0.94˚x0.94˚); 95 levels	MPIOM1.63 Approximately 0.4˚; 802 x 404 longitude/latitude; 40 levels	500
MRI-ESM2-0	Japan	MRI-AGCM3.5 TL159 (~120km); 80 levels	MRI.COM4.4 ~1˚x0.5˚; 360 x 364 longitude/latitude; 61 levels	702
NESM3	China	ECHAM v6.3 T63 (1.9˚x1.9˚); 47 levels	NEMO3.4 Primarily 1˚; 384 x 362 longitude/latitude; 46 levels	300
NorCPM1	Norway	CAM-OSLO4.1 ~2.5˚x2; 26 levels	MICOM1.1 1˚; 320 x 384 longitude/latitude; 53 levels	500
NorESM1-F	Norway	CAM4 ~2.5˚x2˚; 32 levels	MICOM 1˚; 360 x 384; 70 levels	200
NorESM2-LM	Norway	CAM-OSLO ~2.5˚x2˚; 32 levels	MICOM 1˚; 360 x 384; 70 levels	502
SAM0-UNICON	Republic of Korea	CAM5.3 with UNICON ~1˚x1˚; 30 levels	POP2 1˚; 320 x 384; 60 levels	700
TaiESM1	Taiwan	TaiAM1 0.9x1.25; 30 levels	POP2 1˚; 320 x 384; 60 levels	500
UKESM1-0-LL	UK	MetUM-HadGEM3-GA7.1 N96 (1.875˚x1.25˚); 85 levels	NEMO-HadGEM3-GO6.0 Primarily 1˚ with meridional refinement down to 1/3 ˚ in the tropics; 75 levels	750

Table 2. Estimation of the thermodynamic ENSO influence on equatorial Atlantic SST (K). The influence is estimated based on the regression coefficients calculated for Fig. 3b and composite El Niño and La Niña events. The criterion for the composites is that the DJF Niño 3.4 SST anomalies exceed 1 standard deviation. For each composite, we select the Niño 3.4 SST anomalies from Apr0 through May1 (K; 14 months) and multiply each month with the corresponding regression coefficient (W m^{-2} K^{-1}; Fig. 3b; for the CMIP6 models, we use the regression coefficients calculated separately for each model) to obtain the net surface energy flux. The rate of temperature change is calculated as dT/dt = R/(cp*rho*dz), where R is the net surface energy flux calculated above, cp is an approximate value for the specific heat of sea water (3993 J kg^{-1} K^{-1}), rho is the density of sea water at 20C and 35 practical salinity units (1025 kg m^{-3}), and dz is the depth of the mixed layer, taken to be 50 m. To obtain the temperature dT shown in the table, we integrate over the 14 selected months.

	Dataset		
Type of event	**ERA5**	**NCEP**	**CMIP6 ensemble**
El Niño	0.74	0.44	0.51
La Niña	-0.70	-0.38	-0.47

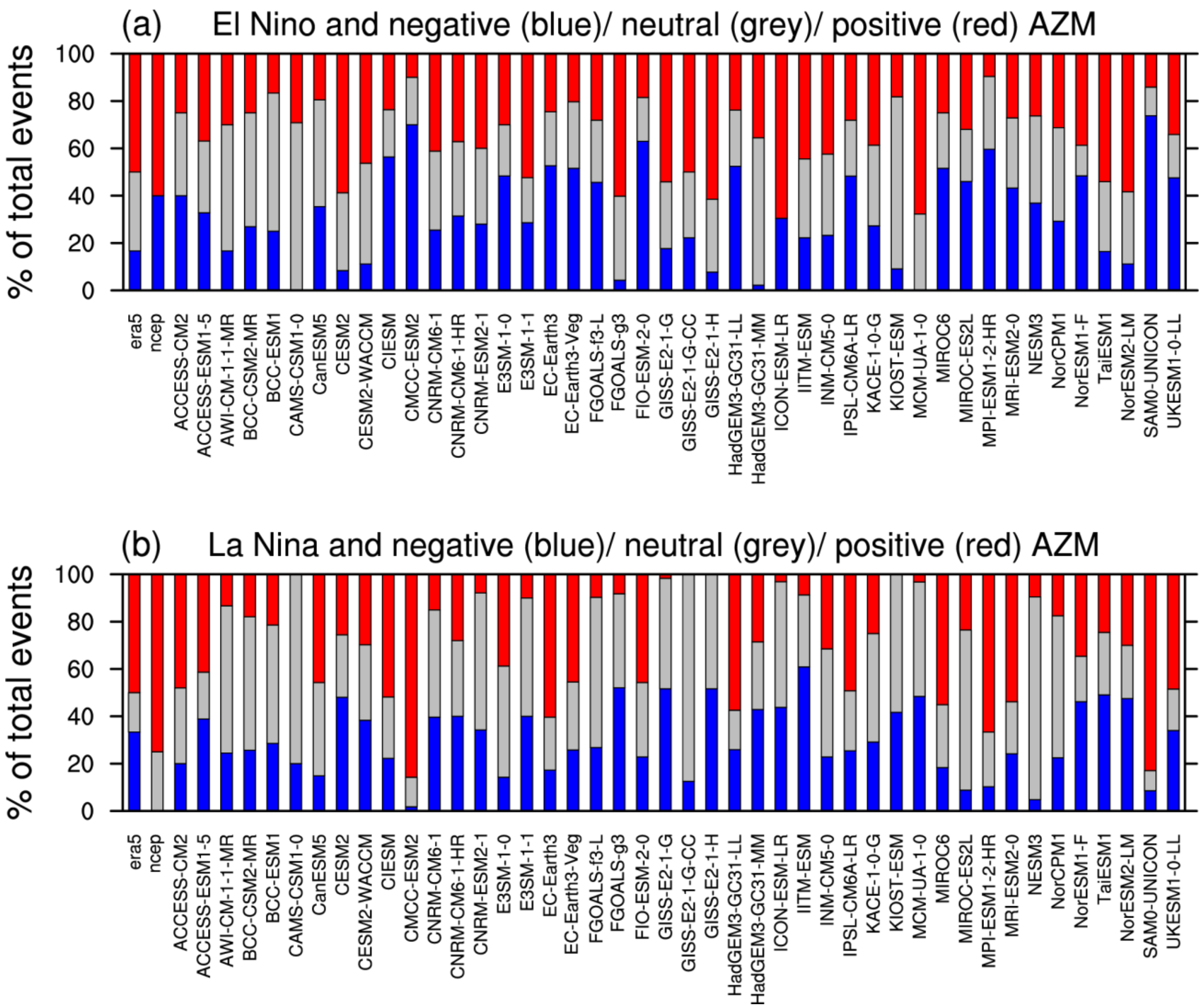

Supplementary Figure 1. (a) Percentage of El Niño events that are followed by AZM- (blue bars), neutral AZM (grey bars), or AZM+ (red bars) for two reanalyses (left most bars) and 44 CMIP6 models. By construction, the three bars add up to 100% for each dataset. (b) Like in (a), but for La Niña events. ENSO events are identified as those years in which the Niño 3.4 index exceeds one standard deviation in DJF.

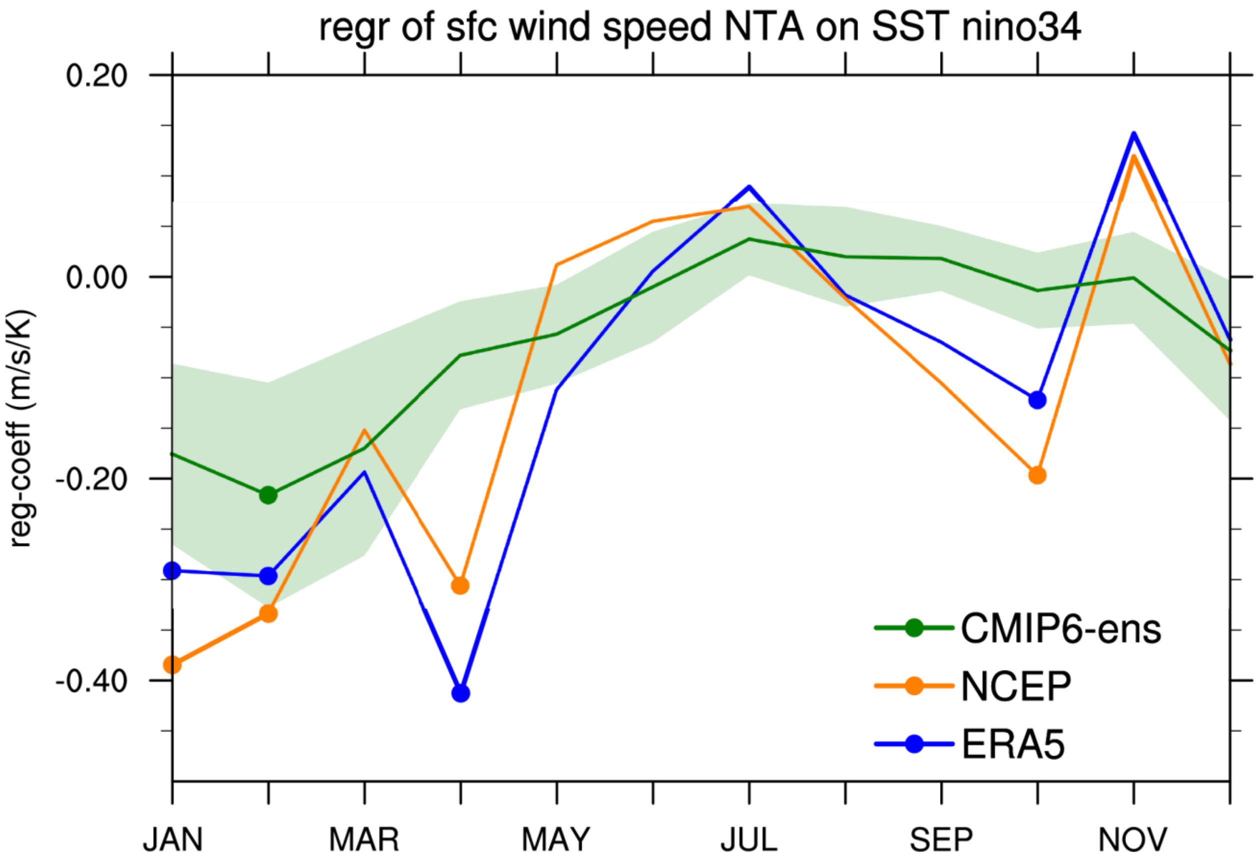

Supplementary Figure 2. Like Fig. 3a but for surface wind speed in the NTA region regressed on the Niño 3.4 index.

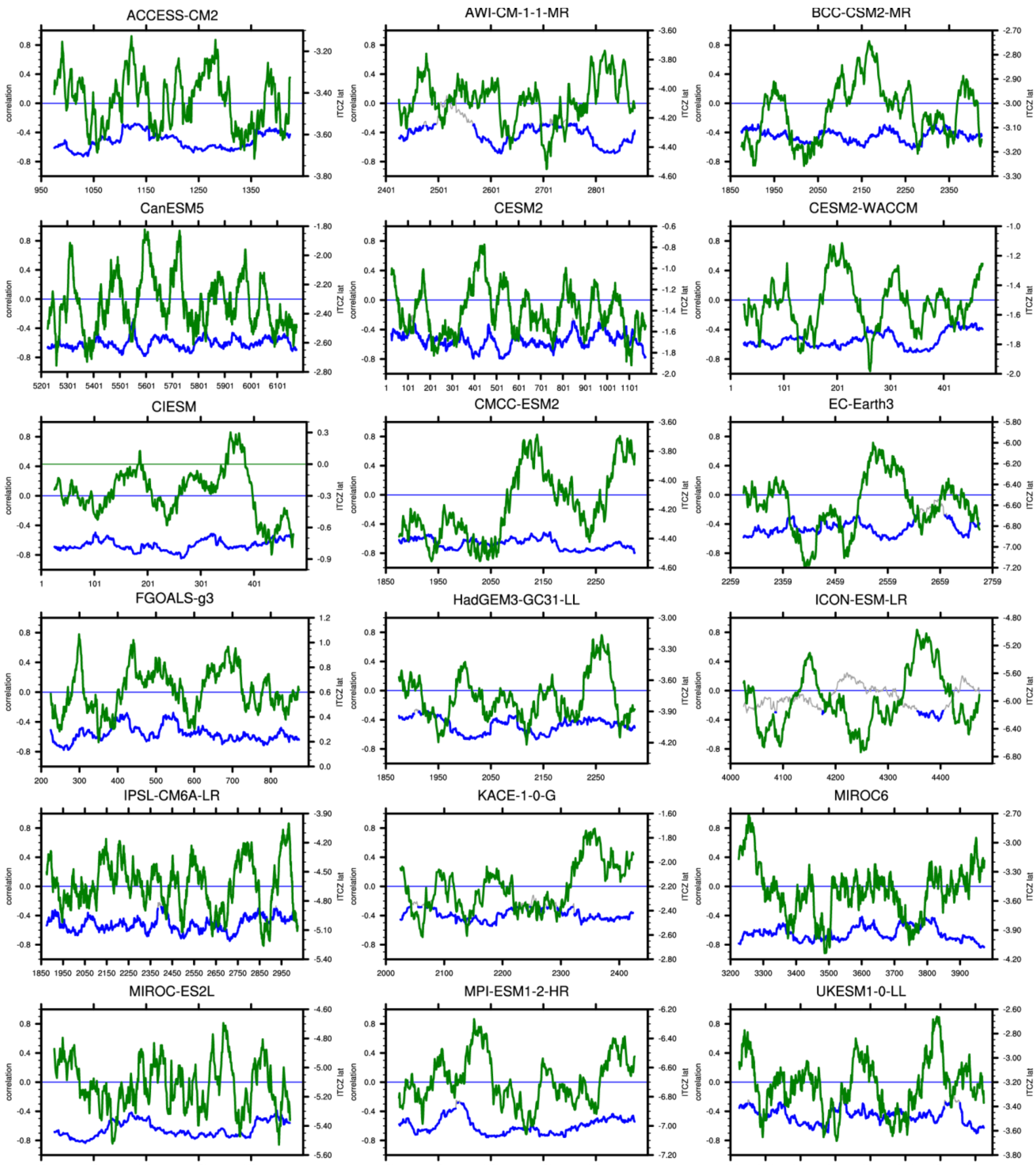

Supplementary Figure 3. Running correlations of the MAM Niño 3.4 SST with the MAM ATL4 surface zonal wind with a 51-year window (blue line; left y-axis), and the latitude of the Atlantic ITCZ, calculated as the latitude of maximum precipitation averaged between 40°-10°W and subjected to a 51-year running mean (green line; right y-axis). 18 selected models are shown.

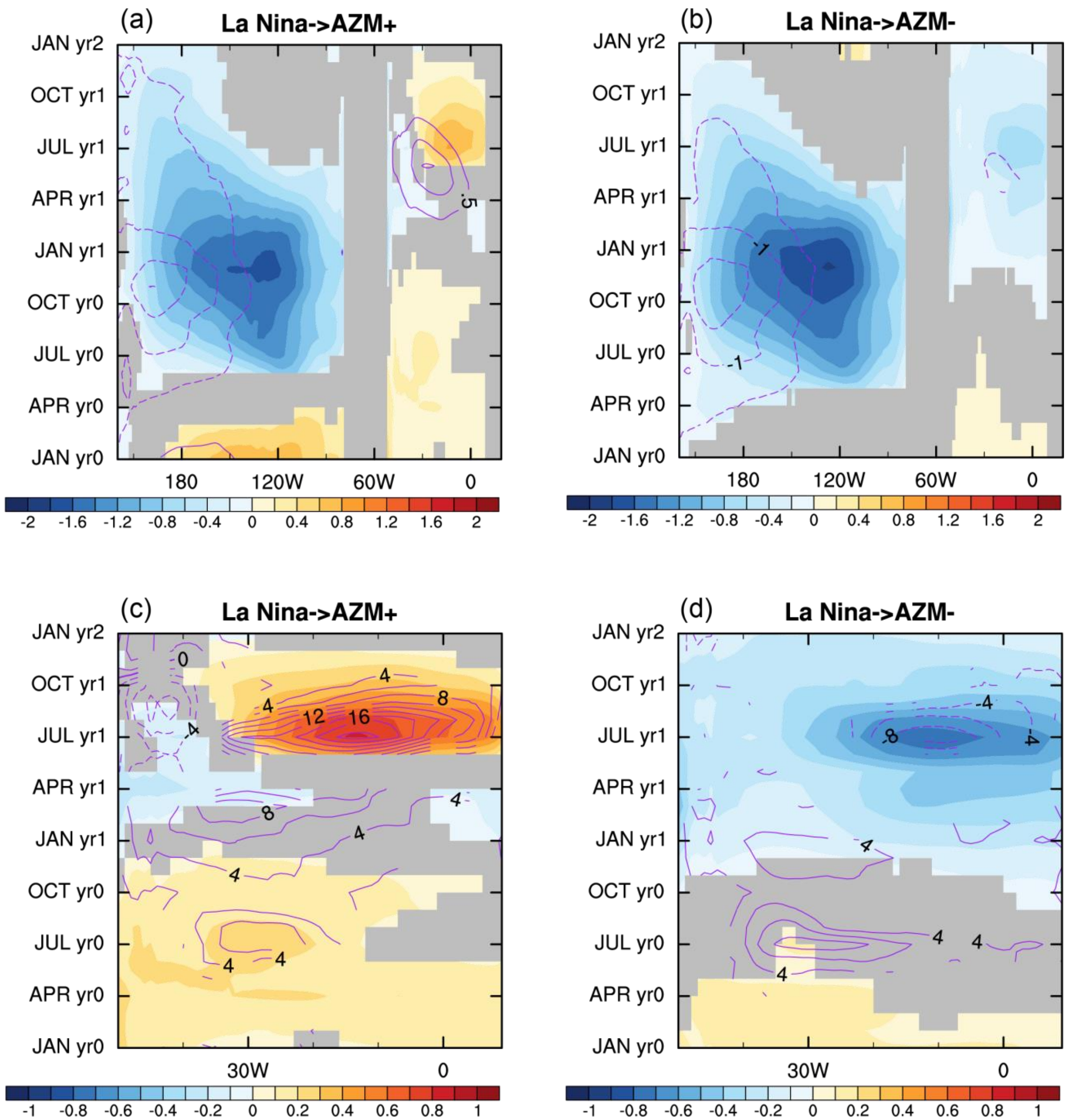

Supplementary Figure 4. Like Fig. 5 but for La Niña events.

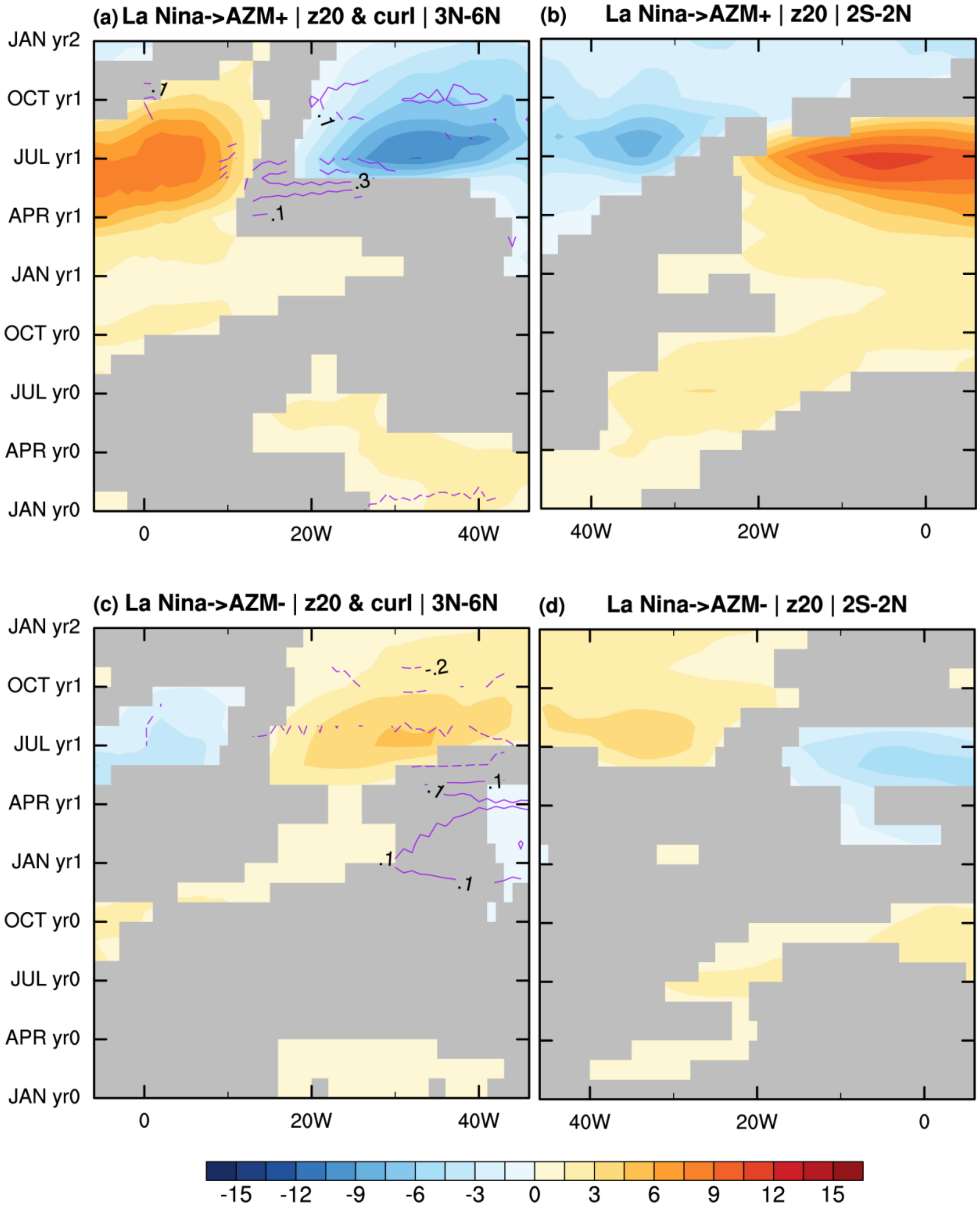

Supplementary Figure 5. Like Fig. 6, but for La Niña events.

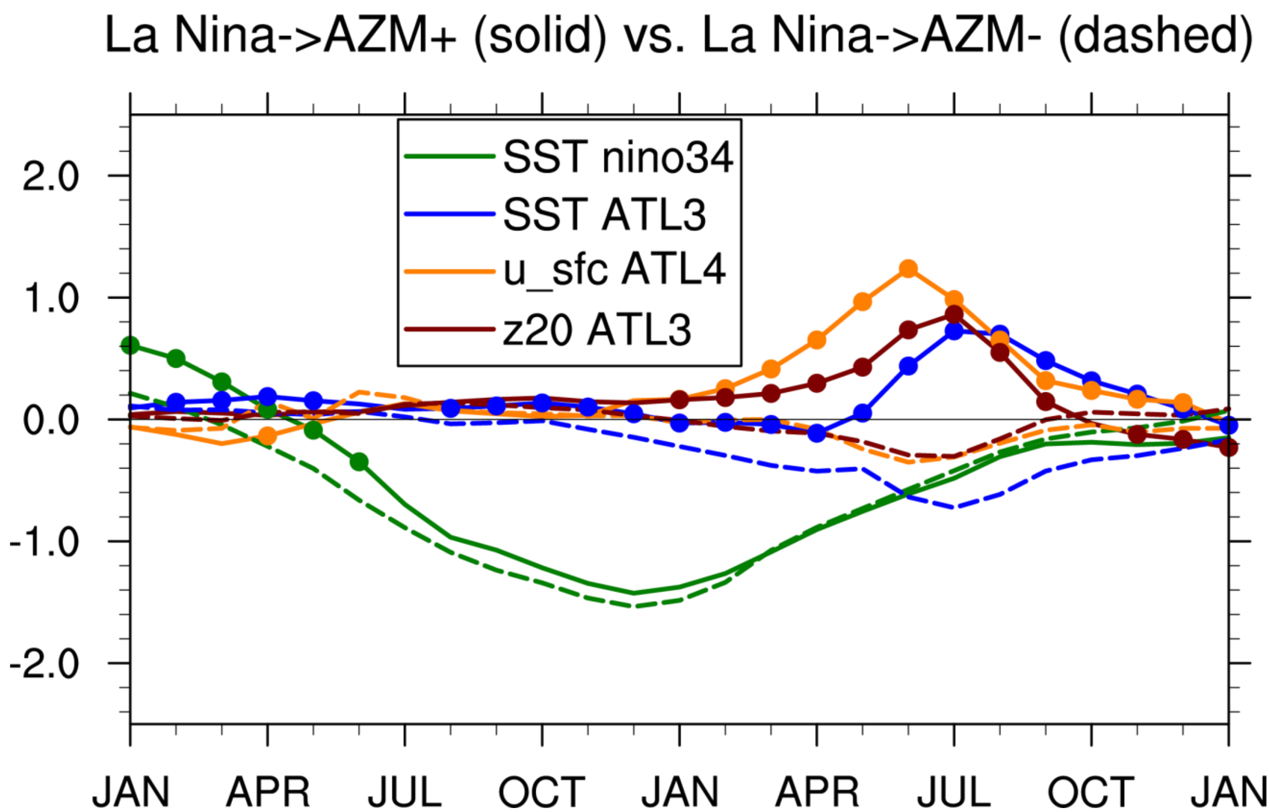

Supplementary Figure 6. Like Fig. 8, but for La Niña events.

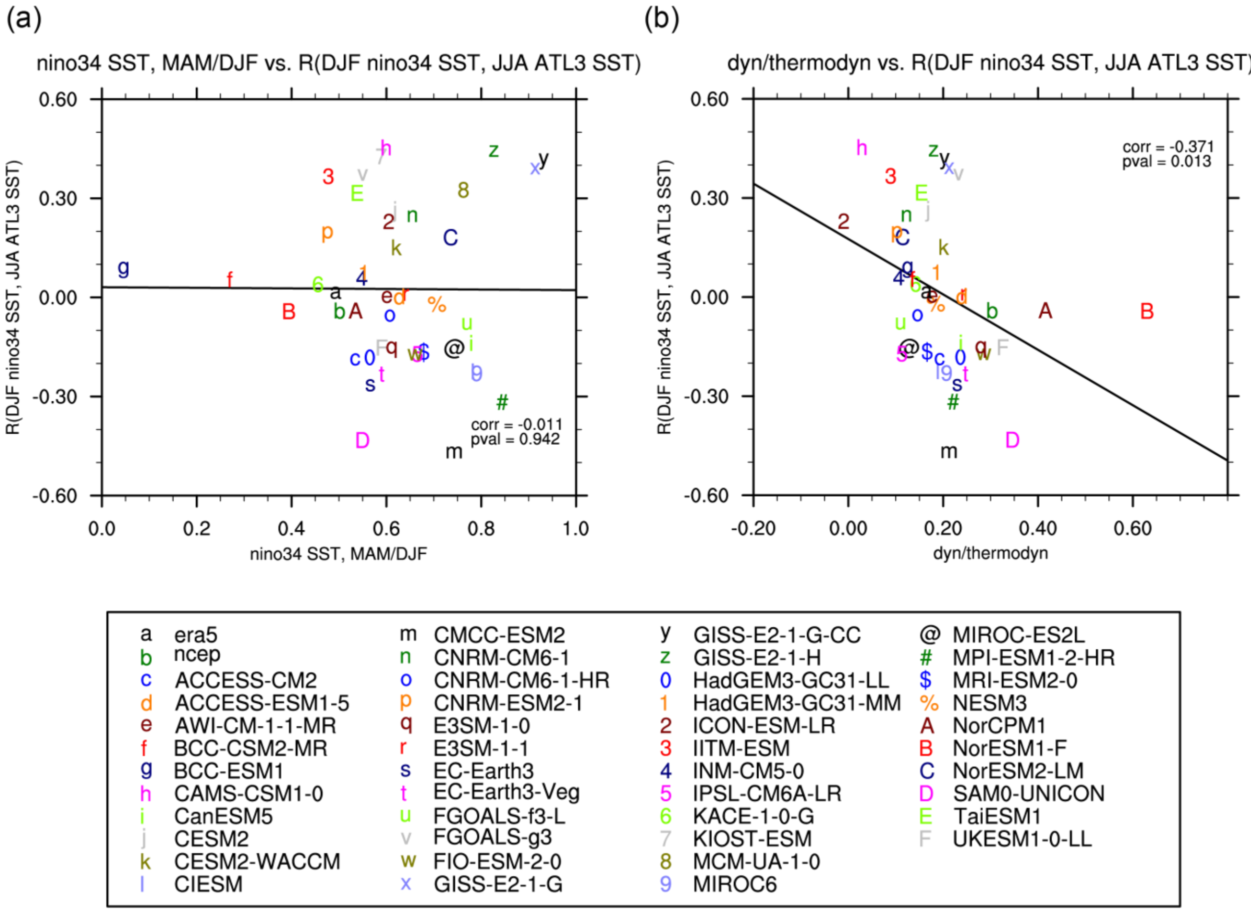

Supplementary Figure 7. Intermodel scatter plots exploring how the ENSO-AZM relation is influenced by ENSO decay speed and by the strength of the dynamic ENSO influence, relative to the thermodynamic influence. The y-axis is the correlation of the DJF Niño 3.4 SST with the following JJA ATL3 SST for each dataset (Fig. 2a). The x-axis shows (a) the Niño 3.4 SST in MAM divided by the Niño 3.4 SST in DJF as a measure for ENSO decay speed, and (b) the ratio of the dynamic over the thermodynamic ENSO influence. The x-axis values in (a) are calculated from ENSO composites, while the ones in (b) are calculated from the regression coefficients for each dataset (Fig. 3b) averaged from April through June of year 1 (dynamic regression coefficients) and September of year 0 through May of year 1 (thermodynamic regression coefficients). The linear regression fit is indicated by a black line in each panel, and the intermodel correlation and its p-value are displayed in the lower right (a) and upper right (b).

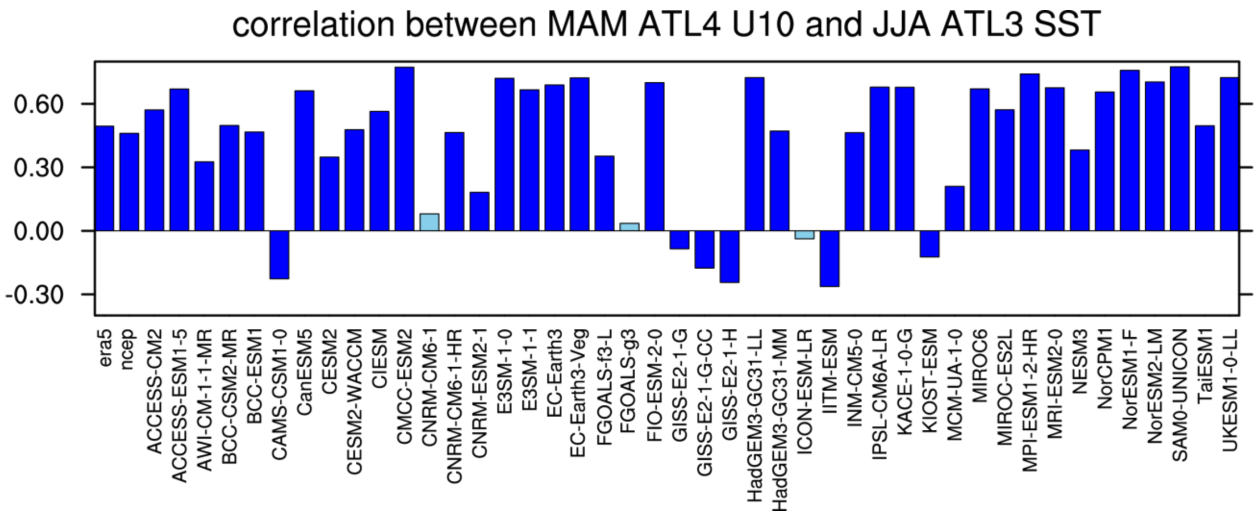

Supplementary Figure 8. Similar to Fig. 2, but for the correlation of MAM ATL4 surface zonal wind with the following JJA ATL3 SST.

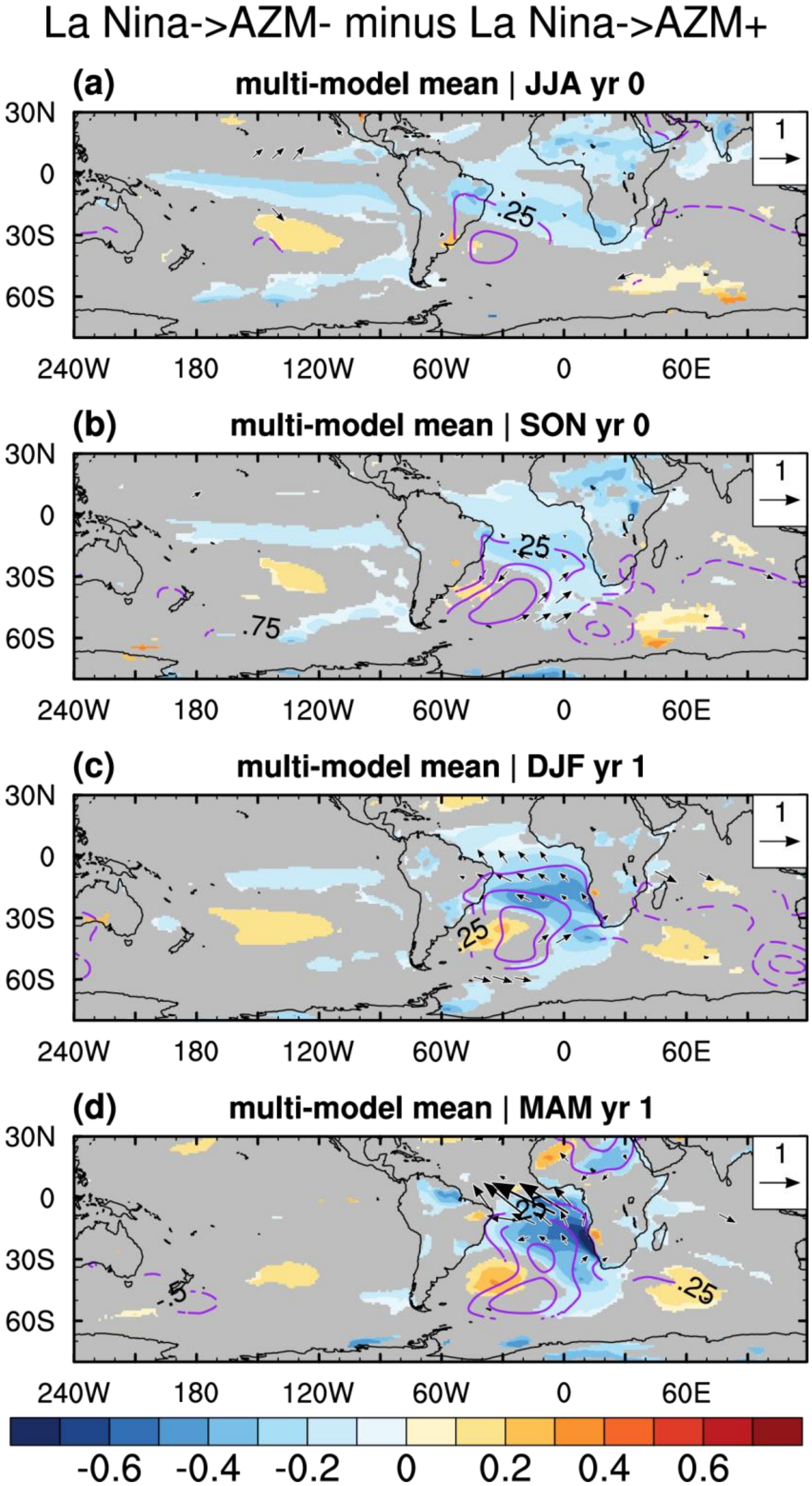

Supplementary Figure 9. Like Fig. 9, but for La Niña events.

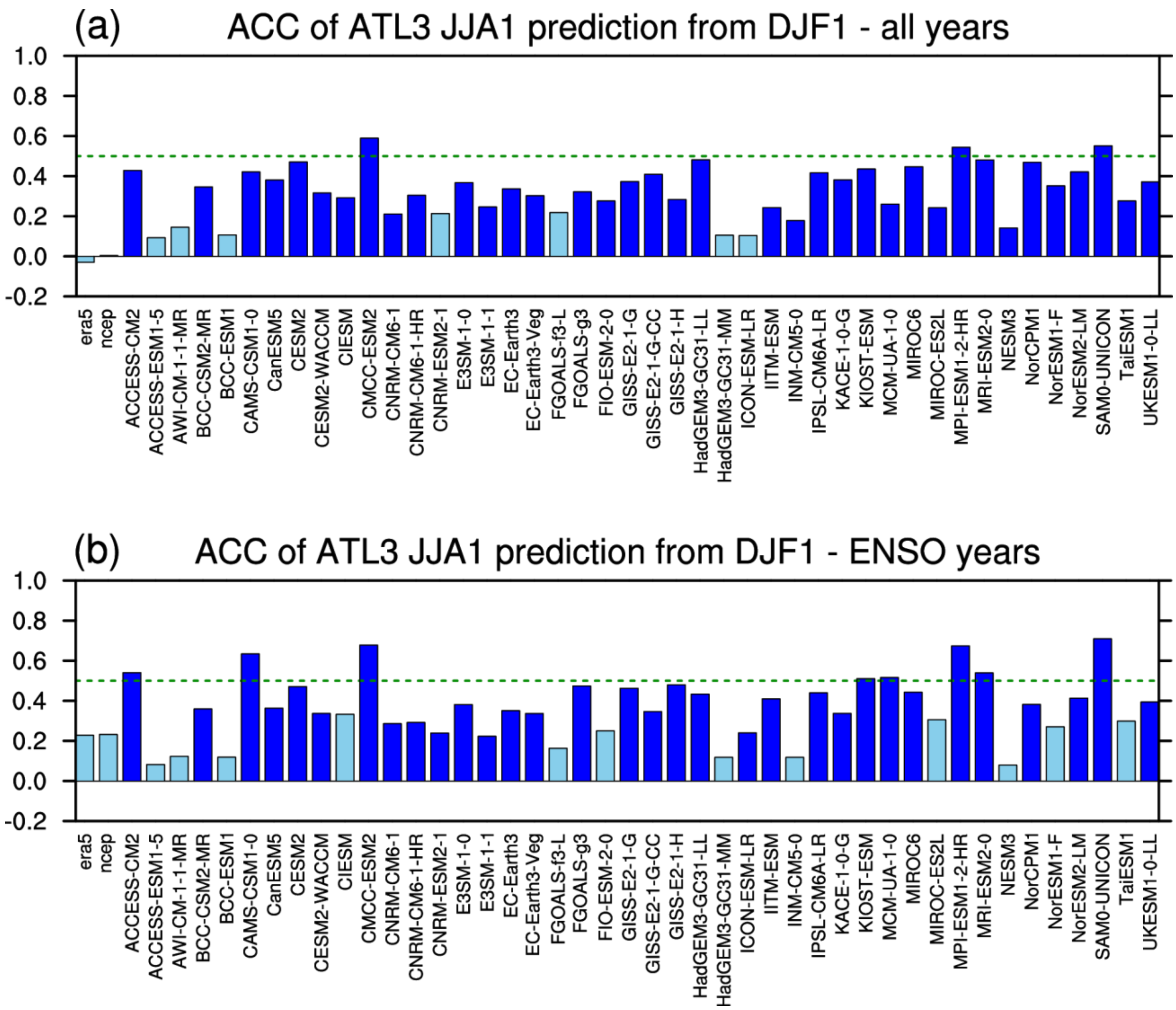

Supplementary Figure 10. Similar to Fig. 11, but with the training period limited to 21 years for all data sets. When the available training data exceeds 21 years (which is the case for all the CMIP6 models), training is performed on consecutive 21-year periods, and the resulting ACC values are averaged using the z-transformation.